Applied Soft Computing 122 (2022) 108883

Contents lists available at ScienceDirect

Applied Soft Computing

journal homepage: www.elsevier.com/locate/asoc

A deep fuzzy model for diagnosis of COVID-19 from CT images☆

Liping Song [a,b,1], Xinyu Liu [a,b,1], Shuqi Chen [a,b], Shuai Liu [a,b,*,2], Xiangbin Liu [a,b,*,2], Khan Muhammad [d,*,2], Siddhartha Bhattacharyya [c]

[a] Hunan Provincial Key Laboratory of Intelligent Computing and Language Information Processing, College of Information Science and Engineering, China
[b] Hunan Xiangjiang Artificial Intelligence Academy; Hunan Normal University, Changsha, 410000, China
[c] Rajnagar Mahavidyalaya, Rajnagar, Birbhum, India
[d] Visual Analytics for Knowledge Laboratory (VIS2KNOW Lab), Department of Applied Artificial Intelligence, School of Convergence, College of Computing and Informatics, Sungkyunkwan University, Seoul 03063, Republic of Korea

ARTICLE INFO

Article history:
Received 19 June 2021
Received in revised form 31 March 2022
Accepted 13 April 2022
Available online 22 April 2022

Keywords:
COVID-19
CT images
Deep learning
Disease prediction
Feature extraction
Fuzzy model

ABSTRACT

From early 2020, a novel coronavirus disease pneumonia has shown a global "pandemic" trend at an extremely fast speed. Due to the magnitude of its harm, it has become a major global public health event. In the face of dramatic increase in the number of patients with COVID-19, the need for quick diagnosis of suspected cases has become particularly critical. Therefore, this paper constructs a fuzzy classifier, which aims to detect infected subjects by observing and analyzing the CT images of suspected patients. Firstly, a deep learning algorithm is used to extract the low-level features of CT images in the COVID-CT dataset. Subsequently, we analyze the extracted feature information with attribute reduction algorithm to obtain features with high recognition. Then, some key features are selected as the input for the fuzzy diagnosis model to the training model. Finally, several images in the dataset are used as the test set to test the trained fuzzy classifier. The obtained accuracy rate is 94.2%, and the F1-score is 93.8%. Experimental results show that, compared with the deep learning diagnosis methods widely used in medical image analysis, the proposed fuzzy model improves the accuracy and efficiency of diagnosis, which consequently helps to curb the spread of COVID-19.

1. Introduction

The coronavirus disease 2019 (COVID-19) that broke out worldwide at the beginning of 2020, has become a global health crisis. Its rapid spread has severely threatened our lives and health. According to Worldometers world real-time statistics, as of 7:01 Beijing time on December 31, 2021, the cumulative number of confirmed worldwide cases of COVID-19 exceeded 286.72 million, reaching 286,724,405. The cumulative number of deaths was 5.445 million, reaching 5,445,126 [1].

COVID-19 is a highly contagious epidemic. Early detection of cases and treatment in isolation is helpful to control the pace of epidemic on a global scale. Reverse transcription polymerase chain reaction (RT-PCR) is the most common method to detect the nucleic acid of COVID-19. Positive nucleic acid detection by real-time fluorescent RT-PCR is a criterion for the diagnosis of COVID-19 [2]. However, this nucleic acid detection method is affected by environmental factors such as specimen sampling, detection process, and detection reagent. In most cases, this method has some false positives and the waiting time for results is too long. Through the summary of the cases, it is found that imaging features of the patients with COVID-19 can also be treated as a diagnostic criterion. As a convenient and advanced medical imaging technique, CT plays a key guiding role in the diagnosis of COVID-19. CT images of early patients show multiple small speckles and interstitial changes, which further develop into multiple ground glass shadows and infiltrating shadows in both lungs. If the disease becomes uncontrolled and severe, lung consolidation may occur. Therefore, the above CT signs can be used to distinguish whether there is a novel coronavirus infection [3].

Since the outbreak of novel coronavirus, several researchers are working on how to quickly diagnose cases. Some of contributors publicly posted a large data set of CT images collected

☆ This work was supported by the Natural Science Foundation of Hunan Province, China with No. 2020JJ4434, Key Scientific Research Projects of Department of Education of Hunan Province, China with No. 19A312; Educational Reform Project of Hunan Xiangjiang Artificial Intelligence Academy, China; Key Research Project on Degree and Graduate Education Reform of Hunan Province, China with No. (2020JGZD025); National Social Science Foundation of China with No. AEA200013.

* Corresponding authors.
E-mail addresses: liushuai@hunnu.edu.cn (S. Liu), xbliufrank@hunnu.edu.cn (X. Liu), khan.muhammad@ieee.org (K. Muhammad).

[1] These authors contribute equally to this paper.

[2] These authors contribute equally to this paper as corresponding authors.

https://doi.org/10.1016/j.asoc.2022.108883
1568-4946/

from various hospitals on COVID-19 cases, which has solved a major problem for researchers and has greatly supported the study methods with data source. For example, Eduardo et al. [4] opened the SARS-Cov-2 CT-SCAN dataset, including 1252 images of patients with positive COVID-19 infection and 1230 images of patients without COVID-19 infection but with other pulmonary diseases. There are 2482 scans in two parts. Zhao et al. [5] constructed an open source COVID-CT dataset, which included 349 images that were positive for COVID-19 and 397 images that were negative for COVID-19. Some contributors have put forward many effective medical classification strategies by studying various classification algorithms. For example, Li et al. [6] used three clinical features to predict the severity of patients with severe COVID-19 infection. The authors screened the electronic archives of nearly 3000 patients to create a prediction model based on the XGBoost machine learning algorithm, which can provide a clinical path to identify critical cases from severe cases and predict the risk of death. Hu et al. [7] put forward a weakly supervised deep learning method to realize detection and classification of COVID-19 and non-COVID-19, which reduced the time required for manual labeling of CT images. Chen et al. [8] used a powerful medical image segmentation system UNet ++ to detect COVID-19. First, the original CT image is input into the trained model. After processing, the prediction box outputs the suspected lesions. The effective regions are then further extracted, and the unnecessary ones are filtered out to reduce false positives. Finally, the effective regions extracted are classified to reduce the rate of missed diagnoses in COVID-19 patients. Shan et al. [9] improved V-Net and proposed a lung tissue segmentation system VB-Net based on deep learning. The system uses a human-in-loop strategy to assist radiologists in segmenting the COVID-19 infected areas to delineate training samples manually and quickly. The data processed by human are handed over to machine learning, and the machine feeds back learning results to human for proofreading to continuously improve the accuracy rate.

In recent years, artificial intelligence has developed rapidly, and intelligent medical technology based on deep learning has made great achievements in the field of medical image processing [10,11]. However, training an ideal deep learning model not only requires huge data-driven analysis tasks, but also consumes a lot of time and memory resources. Therefore, in response to this problem, this paper proposes a deep fuzzy model for analyzing and detecting CT images of people infected with COVID-19. In summary, we have made the following contributions:

(1) A method of feature extraction from CT images using classical deep learning framework is proposed. The COVID-19 and non-COVID-19 CT images are analyzed by using the classical deep learning framework to extract the underlying features of the images. Due to the high-dimensional characteristics of CT images, the extracted low-level features usually contain a lot of redundant information and cannot be classified directly. Therefore, it is necessary to use attribute reduction algorithm to reduce the dimensionality of dense features.
(2) A fuzzy diagnosis model is proposed, which is trained by the processed features of CT images. The model parameters are adjusted continuously to optimize the model performance, to get better diagnosis effect on COVID-19.
(3) The experimental results show that the proposed method is feasible. Compared with the diagnostic method used in literature [5], the classification accuracy of COVID-19 is found to be improved by 5% with the proposed strategy.

The structure of this paper is as follows. Section 2 discusses medical classification technology and fuzzy decision system in detail. Section 3 focuses on feature extraction of CT images used in this paper and construction of the fuzzy diagnosis models. In Section 4, the final experimental results are reported and analyzed by verifying the proposed model on the public dataset. Finally, the outcome of this paper is summarized, and the future work is highlighted.

2. Related work

2.1. Image classification

Image classification is a basic task of computer vision. With the popularity of deep learning, it has become more and more mature. The main realization process is to first obtain the medical image of diagnosed objects through medical imaging equipment. These images are then fed into the trained model. Finally, a diagnostic variable indicating a certain disease or severity level is obtained through analysis [12,13]. Medical image classification is performed using all kinds of medical images, such as computer tomography (CT), magnetic resonance imaging (MRI), X-ray, and ultrasound imaging (UI). Traditional medical classification methods mainly include support vector machine [14], random forest [15], logistic regression analysis [16], and artificial neural networks, [17].

Recently, several scholars have proposed different solutions for medical classification tasks. For example, Chang et al. [18] used SVM to classify breast tumors based on texture features. The classification ability of SVM is basically equivalent to that of a neural network model, but the training time required is much shorter. With the great potential of deep learning being tapped, researchers have turned their research focus to deep learning. The limitation of medical image classification based on traditional neural network method is that the features extracted by artificial design usually have good adaptability for a certain type of disease. For pathological image classification methods that contain diverse changes, deep learning-based methods can learn more generalized feature representation, to adapt to the detection of diverse pathological images in actual diagnosis and treatment scenarios. Therefore, using deep learning to classify medical images has gradually become a research hotspot. Carneiro et al. [19] used the CNN pre-trained by ImageNet to classify tumor based on the multi-view of mammography and segmented microcalcification and mass regions, thereby assessing the risk of breast cancer development in patients. Tajbakhsh et al. [20] used massive-training artificial neural networks (MTANNs) and CNN to detect lung nodules in lung CT images to distinguish between benign and malignant lung nodules. The experimental results show that only when less training data is used, the performance of MTANN is higher than that of CNN. Ayhan et al. [21] used ReNet50, a CNN deep network structure, to classify fundus images. Before classification, the traditional data enhancement method is used to expand the dataset, thus improving the classification accuracy. Roy et al. [22] proposed a new deep network that can simultaneously predict the severity score of the disease associated with the input box and provide the location of pathological artifacts under weak supervision. The transformer model proposed by Shome et al. [23] effectively distinguishes COVID-19 from normal Chest X-rays. More recently, Shankar et al. [24] proposed the BMO-CRNN model for detecting and classifying the presence of COVID-19 from Chest X-ray images.

2.2. Fuzzy decision system

Fuzzy inference system (FIS) is an inference method based on fuzzy rules, which is used to model uncertain and imprecise information. When the knowledge is uncertain, the fuzzy system can use the if-then fuzzy rules to express the knowledge. At

present, fuzzy systems have shown unique advantages in the fields of medical diagnosis, decision analysis, pattern recognition, and automatic control [25]. For example, for the selection of industrial sites, Rikalovic et al. [26] combined a geographic information system for generating location selection with a hierarchical neuro-fuzzy method for site classification and proposed a novel intelligent decision support system. Experiments prove that the proposed method provides accurate results for industrial site classification. Sousa et al. [27] proposed a decision support system based on fuzzy clustering, fuzzy modeling, and fuzzy fingerprints, which provided the corresponding treatment plan according to specific situation of each critical patient and improved the prognosis of patients in the Intensive Care Unit (ICU). Liu et al. [28] proposed a fuzzy decision evaluation model for curriculum performance evaluation. Firstly, the fuzzy evaluation value is obtained by combining fuzzy semantic variables with fuzzy operation, and then the priority result is obtained by using fuzzy sequence method. Finally, the students are compared and analyzed by using triangular fuzzy graph. Based on decision domain theory, Song et al. [29] proposed a hesitant fuzzy decision field theory. The validity of this method is proved by applying it to the problem of route selection in the Northwest Passage of Arctic. Xiao et al. [30] established a fuzzy decision model based on the principle of fuzzy maximum membership by combining theories and methods related to fuzzy decision making. This model explores how to transform qualitative analysis of disease diagnosis into quantitative analysis more satisfactorily, to further eliminate doctors' subjective diagnosis factors and better improve diagnosis efficiency. Casalino et al. [31] proposed a hierarchical fuzzy reasoning system (HFIS) for predicting the risk level of cardiovascular disease, which uses non-invasive technologies to collect vital signs to obtain fuzzy rules for reasoning. By comparing FIS and HFIS, it is observed that the HFIS has higher classification performance. Khomeiny et al. [32] used the Mandani fuzzy method to construct a fuzzy reasoning system that provides teachers with scoring suggestions. The system took students' test scores and students' behavior scores as input, and output suggestions by combining fuzzy rules obtained from artificial summaries.

2.3. Feature extraction and selection

In computer vision and image processing, feature extraction is the basis for subsequent learning and generalization steps. Feature selection selects the most representative features with good classification performance from original extracted features to achieve the purpose of dimensionality reduction. Image feature extraction and selection, as a key link of image classification and recognition, has been applied to several fields related to intelligent systems, such as data mining, anomaly detection, and bioinformatics, which have attracted more and more attention from scholars at home and abroad.

To reduce the computational cost of feature extraction, Abdulhussain et al. [33] put forward a new system to calculate transformation features of images or video frames, which represented the local visual content of images and video frames with these features. The authors compare their proposed method with the traditional extraction method using standard image technology. Compared with the traditional algorithm, their algorithm greatly reduces the computational cost. Chahid et al. [34] proposed a method of feature extraction, which is based on quantization of position weight matrix to carry out multi-class classification to improve the interpretation of biomedical signals. This method verifies the effectiveness on recognition of surface EMG signals of eight different gestures. Martins et al. [35] used feature extraction methods to obtain data that could indicate the incidence of lymphoma to obtain higher lesion classification results. Fractal features were extracted from a RGB model, laboratory model, and color channel, and then the fractal features were spliced into feature vectors. Finally, the authors used the Hermite polynomial classifier to evaluate the performance of their method, which provided good result.

Feature selection technology is mainly divided into filter-based, wrapper-based, and embedded technology. Bennasar et al. [36] proposed two nonlinear feature selection methods, i.e., joint mutual information maximization and normalized joint mutual information maximization used to solve the problem of overestimation of feature importance. The authors compared the proposed methods using 11 publicly available data sets and 5 competing methods. The results show that this method makes the best trade-off between accuracy and stability. The wrapping method selects several features each time according to the objective function, until the best subset is selected. Morphological features do not show obvious value in identifying autism spectrum disorder (ASD). Zheng et al. [37] used similarity to structure multi-feature-based networks (MFN), and then submitted it to a SVM classifier to classify different individuals. The experiments showed that MFN significantly improves the accuracy of distinguishing autism spectrum disorder from typically developing controls (TDC). The embedding method first uses machine learning algorithms (such as lasso regression) and models for training to obtain the weight coefficients of each feature, and the features are selected according to the coefficients from largest to smallest. Kang et al. [38] have designed a new tumor classification method—least absolute shrinkage and selection operators and generalized multi-class support vector machines (rL-GensVM), which use the relaxed Lasso to select genes on the training set. rL-GensVM was used as the classifier. Finally, the experiment shows that the method selects fewer feature genes, and the classification accuracy rate is higher.

3. Materials and methods

Our main goal is to improve the accuracy of COVID-19 diagnosis to control the rate of transmission. In this section, we discuss the materials used in this paper and our proposed method. The dataset used for our model is first described. Then the method of feature extraction and the whole process of feature extraction are introduced. Finally, a fuzzy classifier for diagnosing COVID-19 is constructed. The framework of our method is shown in Fig. 1.

3.1. Materials

During the outbreak of COVID-19, the daily COVID-19 image data from major hospitals was quite huge. However, due to the complexity and diversity of data, it took a lot of time to sort it out. Thus, only few complete and comprehensive COVID-19 image datasets were made available to researchers. The protection of patient privacy was also a factor for data protection. As the epidemic developed more and more serious, people's attention to the virus increased. All kinds of information and data about the epidemic are being constantly updated. At present, there are a small number of public COVID-19 image datasets that support the latest progress of artificial intelligence technology. The image modalities mainly include CT and X-ray, such as MosmedData [39], COVID-19-CT-CXR [40], COVID-19 Radiography Database [41], and SARS-CoV-2 CT-Scan DataSet [4].

The experimental data in this paper has been used from the COVID-CT-Dataset (https://github.com/UCSD-AI4H/COVID-CT), an open-source CT image dataset by Zhao et al. [5]. The source of image is mainly the COVID-19 related publications in journals such as NEJM, JAMA, Lancet, medRxiv, and bioRxiv. The authors

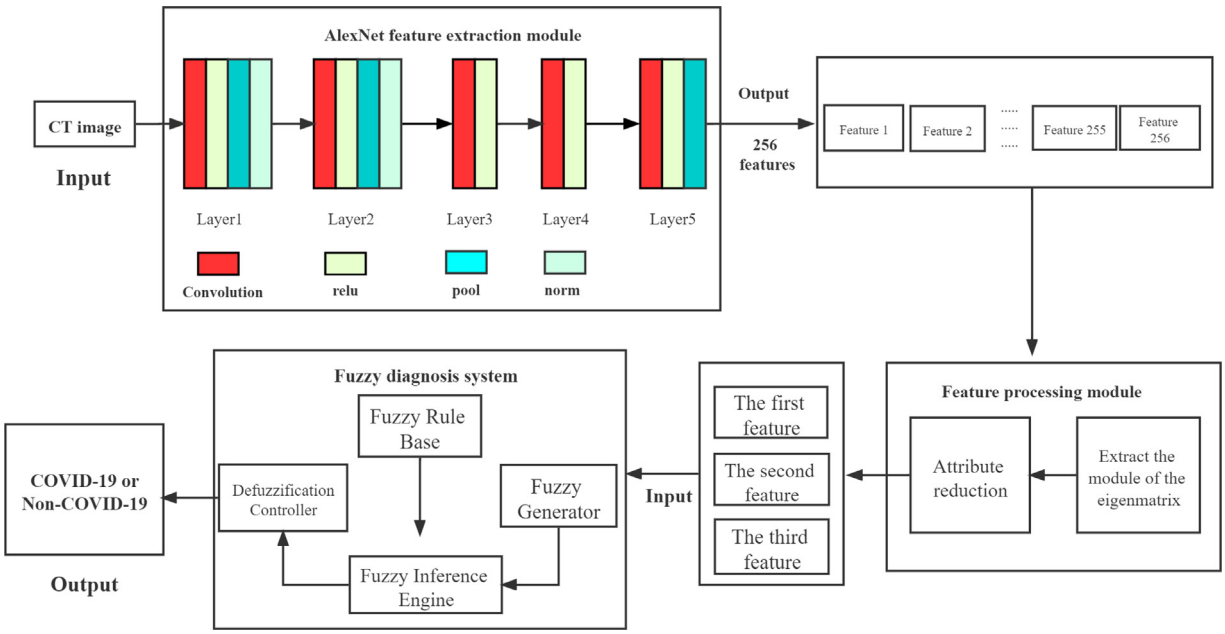

Fig. 1. Framework of the proposed COVID-19 deep fuzzy model.

used Pymupdf to extract the underlying structural information from the preprint PDF files located for all the embedded images. The CT images of the dataset are not CT DICOM images in the true sense, but the author of this dataset has proved through experiments that it does not affect the final diagnosis results. This dataset contains 349 CT images from 143 patients with COVID-19, and 397 images with negative COVID-19. The size of the dataset is not uniform, with an average height of 491, a maximum height of 1853, and a minimum height of 153. The average width, maximum width, and minimum width are respectively 383, 1485, and 124. Fig. 2 shows some examples of a CT image of this dataset. We randomly select 500 CT images from the dataset for training the fuzzy classifier, including 300 COVID-19 CT images and 200 non-COVID-19 images. The test set comprises randomly selected 60 COVID-19 images and 60 non-COVID-19 images from the remaining dataset to verify the validity of the proposed model.

3.2. Methods

3.2.1. Feature extraction

Assuming that we are given any image, the feature extraction method can extract useful information, such as the number, vector, and symbol of image of the "non-image" representation. This process is feature extraction. The extracted "non-image" representations or descriptions are features, which are used to distinguish objects of different classes. To identify the category of the images, it is required that selection of features can not only describe the images better, but more importantly, it is able to distinguish images of different categories. In the process of distinguishing between COVID-19 and non-COVID-19 images, we perform feature extraction on images of these two categories. The entire extraction process is divided into two steps: extraction of the low-level features, feature dimensionality, and attribution reduction.

Extraction of Low-level Features: Traditional feature extraction includes scale invariant feature transformation (SIFT) [42], histogram of oriented gradient (HOG) [43], and local binary pattern (LBP) [44]. SIFT constructs features by finding key points in different scale spaces and by calculating the direction of key points. HOG composes features by calculating and counting histogram of gradient direction of the local area of an image. LBP describes the local texture features of an image, which has remarkable advantages of rotation invariance and gray invariance. With the development of deep learning, feature extraction through neural network has been widely used. Traditional feature extraction methods are generally designed artificially after a large amount of prior knowledge, while CNN based feature extraction is obtained by autonomous learning of neural networks [45]. It is better than SIFT, HOG and other features that rely on prior knowledge. To extract more expressive features, we use the CNN structure to extract features of the COVID-19 CT images. There are different kinds of CNN architectures used for classification. AlexNet, that won the 2012 image recognition contest, has been adopted as the feature extraction framework [46]. Compared with LeNet, AlexNet solved the over-fitting problem and proposed the idea of making the strides smaller than the size of the pooling kernel. Compared with the subsequent deep learning algorithms, it is the basis for the evolution of all subsequent neural networks. The idea of making the strides smaller than the size of pooling kernel is proposed, so that the output of pooling layer obtained has overlap and coverage, which improves the richness of features and reduces the loss of information. Therefore, AlexNet is selected as the feature extraction framework [47]. AlexNet is composed of 5 convolutional layers for feature extraction and 3 fully connected layers for classification. For the process of extracting features, only the first five convolutional layers are needed. Convolution operation is used for feature abstraction and extraction, which signifies the distinctive difference between CNN and the traditional feature extraction algorithms. The pooling operation is used after the convolution operation for feature fusion and dimensionality reduction. AlexNet uses maximum pooling to avoid the blurring effect of average pooling, thereby retaining the most prominent features. The parameters of each layer are shown in Table 1, and the network structure is shown in Fig. 3. The input image is of dimensions 227 $\times$ 227$\times$3. 256 feature maps with a size of 6 $\times$ 6 are obtained using the following equation.

$$L_0 = F\left(CT, \theta\right), \tag{1}$$

where, $F\left(\cdot\right)$ represents feature extraction operation and θ represents the parameters of the network. CT is the input image.

(a) Positive CT images of COVID-19

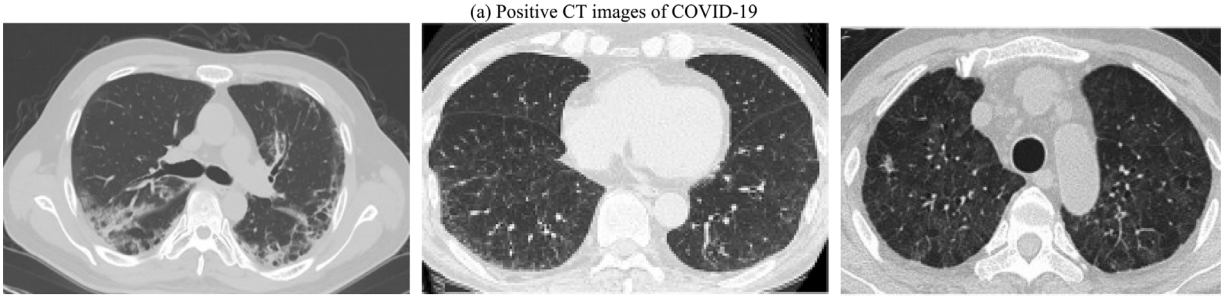

(b) Negative CT images of COVID-19

Fig. 2. Examples of COVID-CT-Dataset.

Table 1
Specific parameters of each layer.

Layer name	Input size	Kernel size	Stride	Pad	In_Chl	Out_Chl	Output size
Conv1	227 × 227 × 3	11 × 11	4	0	3	96	55 × 55 × 96
Maxpool1	55 × 55 × 96	3 × 3	2	0	96	96	27 × 27 × 96
Conv2	27 × 27 × 96	5 × 5	1	2	96	256	27 × 27 × 256
Maxpool2	27 × 27 × 256	3 × 3	2	0	256	256	13 × 13 × 256
Conv3	13 × 13 × 256	3 × 3	1	1	256	384	13 × 13 × 384
Conv4	13 × 13 × 384	3 × 3	1	1	384	384	13 × 13 × 384
Conv5	13 × 13 × 384	3 × 3	1	1	384	256	13 × 13 × 256
Maxpool5	13 × 13 × 256	3 × 3	2	0	256	256	6 × 6 × 256

Feature Dimensionality and Attribution Reduction: Each two-dimensional feature maps are obtained through the feature extraction network. First, it is transformed into a one-dimensional feature vector. Then, we multiply this one-dimensional vector by its transpose to get the modulus of this vector. Through this transformation, we finally obtain 256 feature values from the image. Since the features obtained at this time belong to low-level features of the image, they usually contain a lot of redundant information. Therefore, we need to reduce dense features. The heterogeneous feature subset selection algorithm based on neighborhood rough set of 256 features is used to screen out three features with the strongest expression effect [48] using

$$H = N(L_0, R) \tag{2}$$

where, $N(\cdot)$ represents the subset selection algorithm and R represents the reduction rules. The purpose of this algorithm is to minimize the overlapping area between the classes of a given classification task by searching feature subspace. This is to improve the efficiency of the classification task of COVID-19 based on the selected characteristics. The specific implementation idea is as follows: First, we set the appropriate degree of dependency. The importance of each feature is judged according to dependence. The attribute with the highest importance is selected using forward calculation each time. Then, after removing the selected optimal attributes, the sub-optimal attribute is selected from the remaining attributes, and so on. Finally, the calculation is stopped until the importance of each of remaining attributes is lower than the predefined threshold. According to this method, the experiment selects the three most important features from the 256 low-level features, which constitute the three feature attributes used for training the fuzzy classifier.

3.2.2. Constructing fuzzy decision system

Generally, a complete fuzzy decision system is mainly composed of three parts: fuzzification mechanism, fuzzy rule base, and defuzzification mechanism. The reasoning is completed by combining these three parts. The specific implementation ideas are summarized as follows: First, the precise input value is converted into a fuzzy value that can be processed by the fuzzy system through fuzzification. Then, by combining fuzzy rules in the fuzzy rule library, the fuzzy inference method is used to obtain the inference result. The result obtained at this time is fuzzy, so a defuzzification mechanism is used to convert the fuzzy value into a classical value.

(a) *Fuzzy:* The three features (Feature 1, Feature 2, Feature 3) obtained by feature extraction are expressed as w_i ($i = 1, 2, 3$). They are used as input variables of the fuzzy system. The essence of fuzzification is to fuzzify the given $w_i (i = 1, 2, 3)$, into a fuzzy set $\widetilde{w}_l$. The commonly used fuzzification methods mainly include fuzzy single value method, triangular membership function method, and Gaussian membership function method. In light of the principle of fuzzy control, the fuzzy set representing the membership function must be a convex fuzzy set. In other words, under certain conditions, the membership degree of fuzzy concepts should have a certain degree of stability. By analyzing the selected system feature input value, it can be seen that when the maximum membership function point corresponding to the feature value extends to both sides, its membership degree is monotonically decreasing. Moreover, the triangle membership function can include every state of input and output. Therefore, this paper uses

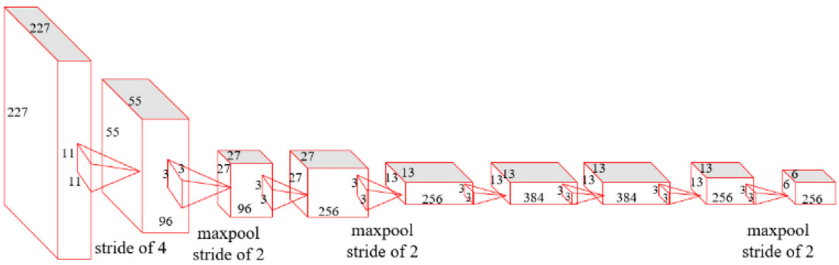

Fig. 3. Network structure used in feature extraction.

the triangular membership function for the fuzzification operation. The specific form is given by

$$\mu_{\tilde{W}}(w) = \begin{cases} 0, & |w - w_i| > \alpha \\ \dfrac{\alpha - |w - w_i|}{\alpha}, & |w - w_i| \le \alpha \end{cases} (\alpha > 0). \quad (3)$$

Here, w represents the given input value and $\widetilde{w}_l$ is the fuzzy set obtained after the fuzzification operation.

(b) *Establishing Fuzzy Rules:* A complete fuzzy inference system is inseparable from the function of fuzzy rules. Fuzzy rules are usually divided into single-dimensional fuzzy rules and multi-dimensional fuzzy rules. Since there are multiple input variables in this paper, and it is necessary to judge the degree of suffering from COVID-19 based on the distribution of multiple feature values, this paper adopts the multidimensional fuzzy rules.
By analyzing the distribution of input variables, we divide the linguistic variables corresponding to features 1, 2, and 3 into NS (negative small), NB (negative big), O (zero), PS (positive small), and PB (positive big). The range of the triangle membership function corresponding to each level is different. Fig. 3 shows the distribution of the membership functions for Features 1–3.
To achieve a better reasoning effect, 125 fuzzy rules are set to restrict the reasoning process according to the number of division levels of the input variables. The specific fuzzy rules are given by

125 fuzzy rules

$$\begin{cases} \textit{if } (\textit{Feature}1 \textit{ is } NS) \textit{ and } (\textit{Feature}2 \textit{ is } NS) \textit{ and} \\ \qquad (\textit{Feature}3 \textit{ is } NS)\textit{, then } (u \textit{ is } NB) \\ \textit{if } (\textit{Feature}1 \textit{ is } NS) \textit{ and } (\textit{Feature}2 \textit{ is } NS) \textit{ and} \\ \qquad (\textit{Feature}3 \textit{ is } O)\textit{, then } (u \textit{ is } NS) \\ \textit{if } (\textit{Feature}1 \textit{ is } NS) \textit{ and } (\textit{Feature}2 \textit{ is } NS) \textit{ and} \\ \qquad (\textit{Feature}3 \textit{ is } PS)\textit{, then } (u \textit{ is } NB) \\ \qquad\qquad \vdots \\ \textit{if } (\textit{Feature}1 \textit{ is } PS) \textit{ and } (\textit{Feature}2 \textit{ is } NB) \textit{ and} \\ \qquad (\textit{Feature}3 \textit{ is } PB)\textit{, then } (u \textit{ is } PB) \\ \qquad\qquad \vdots \\ \textit{if } (\textit{Feature}1 \textit{ is } PB) \textit{ and } (\textit{Feature}2 \textit{ is } PB) \textit{ and} \\ \qquad (\textit{Feature}3 \textit{ is } O)\textit{, then } (u \textit{ is } PS) \\ \textit{if } (\textit{Feature}1 \textit{ is } PB) \textit{ and } (\textit{Feature}2 \textit{ is } PB) \textit{ and} \\ \qquad (\textit{Feature}3 \textit{ is } PS)\textit{, then } (u \textit{ is } PS) \\ \textit{if } (\textit{Feature}1 \textit{ is } PB) \textit{ and } (\textit{Feature}2 \textit{ is } PB) \textit{ and} \\ \qquad (\textit{Feature}3 \textit{ is } PB)\textit{, then } (u \textit{ is } PS) \end{cases}$$

(c) *Defuzzification Mechanism:* This work uses a Mamdani fuzzy inference system. It is the standard model of fuzzy systems. Since the fuzzy processing of the Mamdani fuzzy inference system is performed independently of each component, its parameter setting is simple and clear. The input and output of the system are accurate quantities, so it can be directly applied in actual engineering. So, the output obtained after each rule inference is the distributed membership function of the variable or a discrete fuzzy set. Therefore, after synthesizing the results of multiple rules, the fuzzy set of each output variable needs to be defuzzified. Commonly used defuzzification methods include maximum membership degree method, center of gravity method, and center average method. The center of gravity method can take advantage of all the fuzzy information obtained by inference and can ensure that the accurate value is obtained by processing. Therefore, we use the center of gravity method to defuzzify the inference results (see Fig. 4).

4. Experimental results and analysis

To improve the effectiveness of the proposed method and test the performance of the fuzzy diagnosis system, we have extensively evaluated several commonly used deep learning networks and compared the effects of the two methods. In the next sections, we first introduce the experimental environment and parameter settings, and finally analyze and discuss the experimental results.

4.1. Experimental environment and parameter setting

This experiment includes two parts: feature extraction and fuzzy system training. The experimental environment of feature extraction is based on PyTorch in Windows 10 Home Edition 64-bit system. Hardware includes Intel(R) Core (TM) i5-8300 h CPU processor, NVIDIA GeForce GTX 1060 GPU. The network structure used is AlexNet. The experimental environment of the fuzzy system diagnosis module is a PC with Inter Core 318 TM I5-7500 CPU, 3.40 GHz clock frequency and 64 GB memory, which is implemented on MATLAB 2017.

(1) *Size selection*: When the COVID-9 image is cropped, the characteristics of the lung infection may be lost. But if it is not cropped, the data set size remains inconsistent, and it is difficult to train with deep learning. To ensure the integrity of lungs in the images and make the data meet to the input requirements of the model in this paper, we unify the data size into 227 × 227 through resize operation and set the bit depth of the image to 24. Therefore, the final input size of the model comes out to be 227 × 227 × 3.
(2) *Loss function and optimization function*: The cross-entropy loss function is commonly used in classification models, which can learn the difference from the model and the training distribution. Compared with other losses, the cross-entropy calculation loss can converge to a better local minimum point, thereby improving the accuracy. ReLU (Rectified Linear Unit) is used as activation function. ReLU solves the problem of derivative with activation function, so it helps to alleviate the disappearance of gradient. To a certain extent, it can also alleviate gradient explosions,

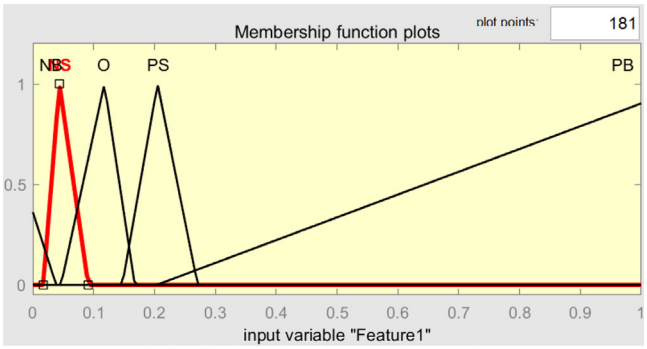

(a) The distribution of membership function for Feature 1

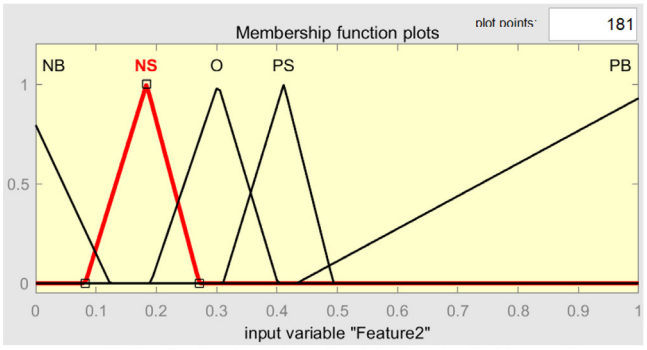

(b) The distribution of membership function for Feature 2

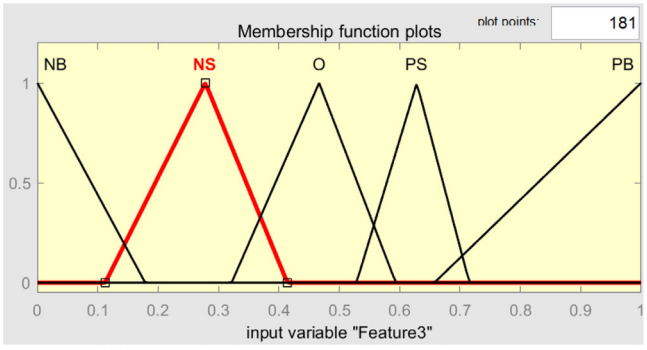

(c) The distribution of membership function for Feature 3

Fig. 4. The distribution of membership function of each feature.

thereby speeding up training. The optimization function used is the Adam optimizer [49], which is used to replace stochastic gradient descent in the deep learning model.

(3) *Others*: When AlexNet is trained for feature extraction, the batch size is taken as 16, the epoch is equal to 1000, and the learning rate is set to 0.0001.

4.2. Analysis about feature extraction

To prove the feature extracted by AlexNet in favor of improving the classification accuracy of the proposed fuzzy model, we discuss and analyze the feature values obtained from the output and the visualization of feature extraction process from two different levels.

Each of the 256 eigenvalues about the image has its own value, and there is an indispensable connection between them. We have randomly selected 10 images in the training set, of which 5 are COVID-19 CT images and 5 are non-COVID-19 CT images. We have performed numerical statistics on the 256 eigenvalues obtained from these 10 images, and analyzed their average, median, standard deviation, numerical range, minimum, and maximum values.

Table 2
Statistical results for features of COVID-19 images.

Number	COV-1	COV-2	COV-3	COV-4	COV-5
Average	0.0553	0.0359	0.0561	0.0501	0.0449
Median	0.0067	0.0027	0.1038	0.0975	0.0072
Standard deviation	0.1194	0.1180	0.1087	0.1037	0.0974
Numerical range	0.9633	1.1978	0.8605	0.8307	0.7827
Minimum	0.0000	0.0000	0.0000	0.0000	0.0000
Maximum	0.9633	1.1978	0.8605	0.8307	0.7827

Table 3
Statistical results for features of non-COVID-19 images.

Number	NCOV1	NCOV2	NCOV3	NCOV4	NCOV5
Average	0.3327	0.2120	0.0893	0.2776	0.0712
Median	0.1201	0.6450	0.0289	0.0869	0.0177
Standard deviation	0.4944	0.4463	0.2129	0.5151	0.1757
Numerical range	3.6407	4.4046	2.4700	4.2698	1.5744
Minimum	0.0000	0.0000	0.0000	0.0000	0.0000
Maximum	3.6407	4.4046	2.4700	4.2698	1.5744

Tables 2 and 3 respectively show the statistical results obtained after these experiments. It can be seen from the Tables that there is a big difference between the two in the average value. The image of COVID-19 is about 0.05 or below, while the image of non-COVID-19 is larger, all above 0.05. The median of the features for COVID-19 is small, generally below 0.01; the median of the features for non-COVID-19 is above 0.01. The standard deviation of the features of COVID-19 is generally around 0.01; the median of the features of non-COVID-19 is above 0.1, mainly around 0.5. For the maximum value, the eigenvalue of COVID-19 generally fluctuates around 0.1. The eigenvalues of non-COVID-19 are all above 1, which is more than 10 times higher. The maximum value of COVID-19 generally fluctuates around 0.1. The minimum value of both is 0, so the eigenvalue of the latter has a much larger numerical span than the eigenvalue of the former. Through the statistics of the feature values, it is found that the feature values of the two categories of images are very different. The two types of images can be completely separated based on this information. Therefore, it shows that the method of extracting features used in this paper is reliable and beneficial for subsequent classification.

To show the process of feature extraction more clearly, we visualize the feature map obtained after each convolutional layer of the model. We selected one CT image of COVID and Non-COVID from Fig. 2 for analysis, and the images obtained are as shown in Fig. 5. Since feature extraction has five convolution layers in the AlexNet, feature maps of different dimensions are obtained after each convolution layer. The number of channels in the first convolution is 96. Each channel extracts a feature according to a certain property of the image, so a total of 96 feature maps of 55×55 is obtained. These 96 features are tiled together in a row of 12 to obtain the feature map for Conv1. The channel number of the second layer convolution is 256. The 256 feature maps of 27×27 are then tiled together in a row of 16 to obtain the feature map for Conv2. According to this step, we obtain the feature maps for Conv3, Conv4, and Conv5, respectively. Low-level features are extracted to high-level features from the feature map of Conv1 to that of Conv5. At the beginning, the texture of the entire image can be clearly seen. By comparing second feature map in (a) and (b) feature map of Conv1, we find that there are significantly more white edges in the middle of the lungs in the COVID-19 CT image. The model pays attention to different characteristics between different types of images in the process of extracting features to obtain correct feature values to improve model performance.

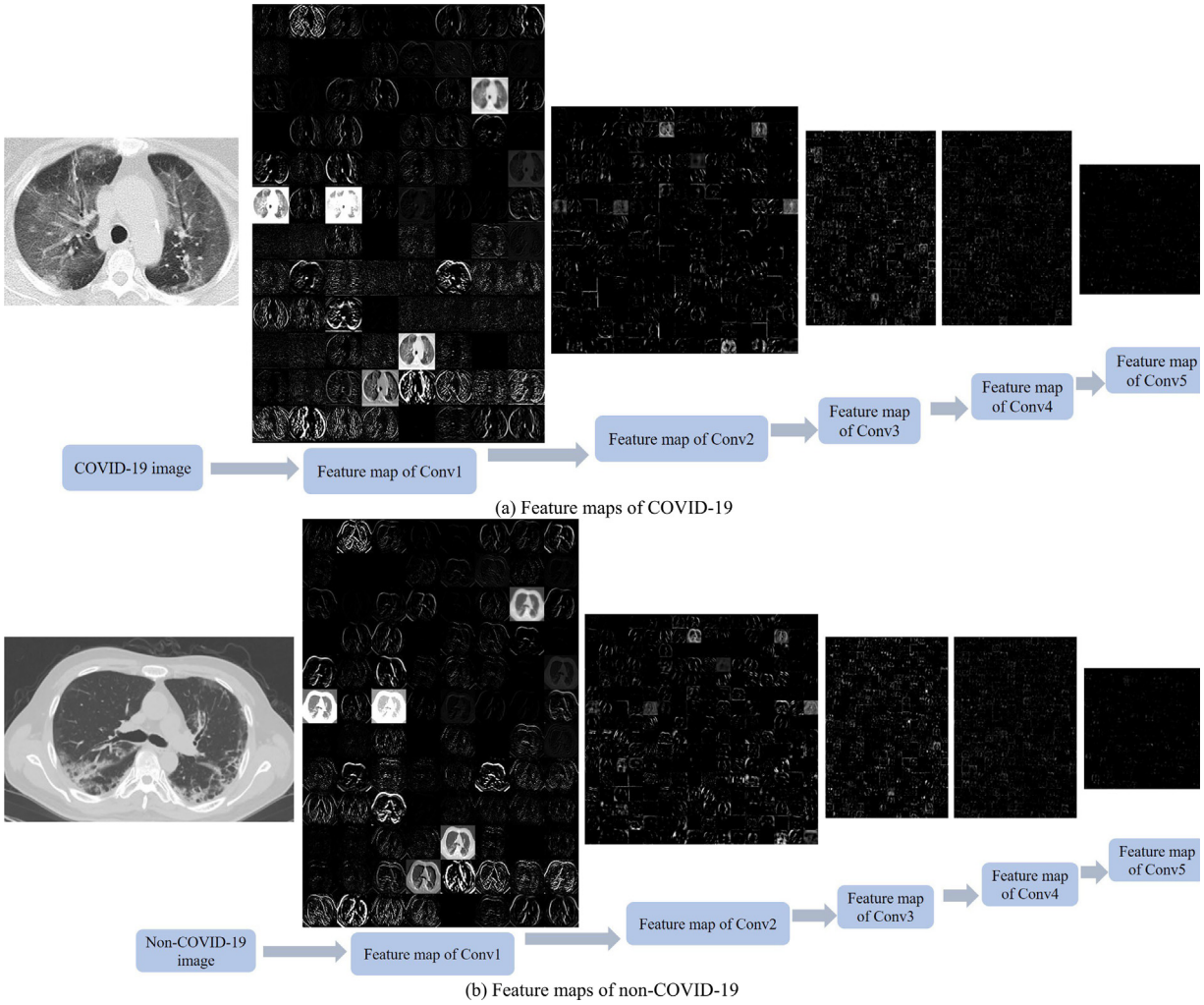

Fig. 5. The feature map obtained by each convolution layer.

4.3. Experimental results and discussion

Throughout the training process of deep fuzzy system, we adjust the parameters through multiple trainings, and then get a stable diagnostic effect. When we train to epoch = 16, the accuracy rate reaches about 94%. Then we train for many times and found that the accuracy rate stabilizes, and the final effect is 94.17%. Fig. 6 is the training curve. We use this proposed model to evaluate the performance of specific tasks through repeated verification. The results obtained on the test set are summarized in Table 4, which includes the confusion matrix for each test image and the performance of this model. From the confusion matrix, we can see that the fuzzy system is able to diagnose all the 60 COVID-CT images with new coronary pneumonia correctly, with the classification accuracy rate of 100%. About the 60 CT images that do not suffer from new coronary pneumonia, 53 of them are correctly diagnosed and 7 are judged to be COVID, and the classification accuracy rate was 88.33%. Four indicators have been used to evaluate the model, which include accuracy (ACC), precision (PRC), recall (REC), and F1-score. Accuracy is used to measure the percentage of diagnostic predictions that are completely factual. Precision is the proportion of true positives contrast predicted positives. The recall reflects the ratio of positive samples being correctly predicted. The higher the recall is, the stronger is the ability of correct diagnosis. The F1-score is the harmonic average of the precision and recall. For all the four indicators, a higher value signifies a better performance. By applying the selected test set to the trained fuzzy diagnosis model, the accuracy is found to be 94.17%, the precision to be 100%, the recall rate to be 88.33%, and the F1-score to be 93.80%. The four evaluation indicators are calculated using

$$ACC = \frac{TP + TN}{TP + FP + FN + TN} \tag{4}$$

$$PRC = \frac{TP}{TP + FP} \tag{5}$$

$$REC = \frac{TP}{TP + FN} \tag{6}$$

$$F1 = \frac{2PRC * REC}{PRC + REC}. \tag{7}$$

Among these, TP is the number of patients without disease in both the real and the predicted results. FP is the number of true outcomes for the disease with prediction of no disease. TN is the number of cases the disease in actual and predicted results. FN is the number of true outcomes for which there is no disease and the predicted outcome for which there is disease.

Among the four indicators, the accuracy reaches 100%, and the recall is the lowest. Under ideal circumstances, we hope that both PRC and REC are as high as possible, but in fact these two are contradictory under certain circumstances. The accuracy of 100% means that the model can ensure that when a positive

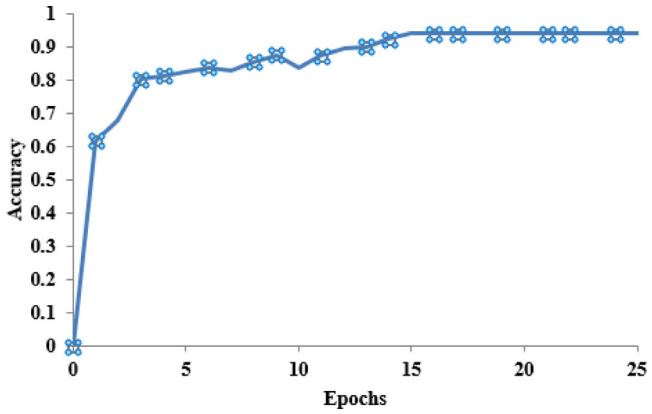

Fig. 6. The training curve of Mamdani fuzzy inference system.

Table 4
The result of testing the fuzzy model on the test set.

Predict	True	
	Non-COVID-19	COVID-19
Non-COVID-19	53	0
COVID-19	7	60
Metrics	Result (%)	
Accuracy	94.17	
Precision	100.00	
Recall	88.33	
F1-score	93.80	

sample is detected, the probability of a positive occurrence is high. But it cannot guarantee that when a negative sample is detected, the diagnosis must be negative. On the contrary, a high recall rate means fewer missed. It can ensure that when the model detects negative samples, the probability of a negative occurrence is high. But it cannot guarantee that when a positive sample is detected, it must be diagnosed as positive. That is, the precision rate measures the accuracy of a model to make a positive judgment, while the recall rate measures the accuracy of a model to make a negative judgment. In the actual medical diagnosis system, we hope to sacrifice the recall rate to improve accuracy. If a person who is not ill is wrongly detected as ill, it can be further ruled out through follow-up inspections. If a person who is ill is detected as not ill, it will delay the opportunity for treatment and may cause serious consequences. Therefore, this model just satisfies this criterion.

Given the small size of the dataset, deep networks are difficult to train in this case and may explode or disappear in gradients. Therefore, the AlexNet model is prone to overfitting, which reduces the generalization ability of the model. If the deep network cannot be trained effectively, the convolutional layer cannot extract useful features, thus reducing the classification accuracy of the model. Table 5 shows the structural comparison of each classical network model. We compared four common classification networks, AlexNet [46], VGG-16 [50], GoogLeNet [51], and ResNet-152 [52] as regards to the network structure, network parameters, and computing power consumed by the model. It can be seen that compared with the others, AlexNet has fewer network layers and convolutional layers, which is in line with the data scale. From the perspective of the model parameters, the parameters of AlexNet are more than half less than VGG, which is equivalent to parameters of ResNet-152. In terms of the amount of computing power required for training, AlexNet is the least, and ResNet-152 is more than ten times of that. Finally, we choose the most suitable AlexNet for feature extraction.

Table 5
Structure comparison of classical network models.

Model	AlexNet	VGG-16	GoogLeNet	ResNet-152
Layer number	8	16	22	152
Layer number of convolutions	5	13	21	151
Parameter numbers/Million	60M	138M	6.9M	60M
Floating point operations/billion	1.5B	15.3B	2B	11.3B

In the experiments, we have also compared the general deep learning model and the fuzzy model proposed in this paper from classification indicators. The experimental results are shown in Table 6. Three types of deep learning diagnostic models are chosen viz., VGG-16 [50], ResNet-50 [52], EfficientNet-b1 [53], DenseNet-121 [54], DenseNet-169 [54], and DenseNet-169 (TL + CSSL). Both DenseNet and ResNet-50 are large-scale networks that improve accuracy by deepening the network layer. But as the network deepens, the problem that arises is that the gradient disappears, especially if the data volume is small. Compared with the three types of deep networks, the fuzzy diagnosis system has improved accuracy by 18%, 15% and 17%, respectively. To solve the problems mentioned above, the network added training strategy of transfer learning. It helps to learn the target task by using the large image set and its class labels in the source task. The benefits of transfer learning can be significant in some cases. Densenet-169 (TL + CSSL) is the result of Densenet-169 being pre-trained on ImageNet by transfer learning (TL) [55] and then fine-tuning with contrastive self-supervised learning (CSSL) using the COVID-CT dataset [56]. DenseNet-169 (TL + CSSL) is the best performer among several deep learning frameworks, which is about 10% higher than DenseNet-169 trained from scratch. However, there is still room for improvement in accuracy compared to the fuzzy diagnostic systems. In addition, we also compared the proposed model with existing research on the detection of COVID-19 diagnosis in CT images through deep neural networks. The CNN-based CAD system uses a multi-layer method to extract the most unique features of the pattern [57]. The feature extraction process usually requires a lot of labor and time. DRE-Net integrates the pre-trained ResNet50 with the Feature Pyramid Network, and inputs it into multi-layer perception for image-level prediction [58].

Based on the same dataset, we found that the proposed model is superior to the other three models in terms of accuracy, F1 score, and AUC. To further verify the generalization of the model, we performed same validation on SARS-COV-2 CT-SCAN dataset [4]. Deep learning requires a large data for training to restrain over-fitting. These data are more favorable for fuzzy models. Compared with the best model in deep learning, DenseNet-169 (TL + CSSL), our model has an accuracy improvement of more than 5%. The training time is also greatly reduced. Thus, it is confirmed through experiments that a model with this performance has greater clinical value. The deep fuzzy system based on artificial intelligence can quickly identify the microscopic information and key features of lesions. By screening and extracting characteristic information of the disease from massive data to make disease diagnosis, the ability of CT in the early diagnosis of COVID-19 and its differential diagnosis ability from other pneumonia can be improved. In this way, the prognosis of patients can be improved. The incidence of critical cases and mortality can be reduced, and the corresponding treatment can be done early in clinical practice.

5. Conclusion

Novel coronavirus is the first new coronavirus strain discovered in 2019. Its transmission speed is beyond our imagination.

Table 6
Results of fuzzy model are compared with those of other models.

Model	Positive training data	Accuracy (%)	F1-scoe (%)	AUC (%)
VGG-16 [50]	COVID-CT-349	76.0	76.0	82.0
ResNet-50 [51]	COVID-CT-349	77.4	74.6	86.5
EfficientNet-b1 [53]	COVID-CT-349	79.0	79.0	84.0
DenseNet-121 [54]	COVID-CT-349	79.0	79.0	88.0
DenseNet-169 [54]	COVID-CT-349	79.5	76.0	90.1
DenseNet-169 (TL+CSSL)	COVID-CT-349	89.1	89.6	98.1
Self-supervised learning of transfer learning [59]	COVID-CT-349	86.0	85.0	91.0
CNN-based CAD system [57]	60 infected patients of CT COVID-19	90.3	87.1	97.6
DRE-Net [58]	88 infected patients of CT COVID-19	86.0	87.0	95.0
CovNNet [60]	121 CXR image	87.1	–	–
Fuzzy model (Ours)	SARS-CoV-2 CT-scan [4]	**91.7**	**91.3**	**96.4**
Fuzzy model (Ours)	COVID-CT-349	**94.2**	**93.8**	**97.4**

It has the characteristics of long survival time and wide transmission routes. To safeguard world public health security, we have explored available knowledge in the field to develop new models for enhancing the capacity of response to epidemics. We have designed a fuzzy model for COVID-19 diagnosis in this study. COVID-19 is quickly classified by using the open COVID-CT-Dataset, which has practicability for research. Our model can accurately diagnose the COVID-19 and non-COVID-19 cases, and the time required is also less. Therefore, the problem about shortage of medical resources has been alleviated, the speed of diagnosis has been accelerated, and more treatment time has been unearthed for patients with COVID-19. Experimental results show that the proposed model has higher classification accuracy and F1-score. Compared with the general deep learning models and related state-of-the-art methods, the proposed model has significantly improved speed and accuracy.

Although medical image processing technology has reached a quite mature level, there are still a lot of challenges and problems to be explored for precise prevention of large-scale epidemics. The proposed fuzzy model for the diagnosis of COVID-19 is relatively simple in terms of function, although it increases the treatment time for patient's diagnosis. Methods, however, remain to be investigated to classify the severity of infection in patients as well as the classification of the infected areas. The authors are currently engaged in this direction.

CRediT authorship contribution statement

Liping Song: Conceptualization, Software, Writing - original draft. **Xinyu Liu:** Conceptualization, Software, Writing - original draft. **Shuqi Chen:** Conceptualization, Validation. **Shuai Liu:** Methodology, Project administration, Writing - review & editing. **Xiangbin Liu:** Methodology, Supervision. **Khan Muhammad:** Investigation, Writing - review & editing, Supervision. **Siddhartha Bhattacharyya:** Investigation. All authors contributed to writing and reviewing.

Declaration of competing interest

The authors declare that they have no known competing financial interests or personal relationships that could have appeared to influence the work reported in this paper.

References

[1] Covid-19 coronavirus pandemic, 2021, Retrieved from https://www.worldometers.info/coronavirus/.

[2] Meagan N Esbin, Oscar N. Whitney, Shasha Chong, Anna Maurer, Xavier Darzacq, Robert Tjian, Overcoming the bottleneck to widespread testing: a rapid review of nucleic acid testing approaches for COVID-19 detection, Rna 26 (7) (2020) 771–783.

[3] Shuchang Zhou, Yujin Wang, Tingting Zhu, Liming Xia, Ct features of coronavirus disease 2019 (COVID-19) pneumonia in 62 patients in Wuhan, China, Amer. J. Roentgenol. 214 (6) (2020) 1287–1294.

[4] Plamen Angelov, Eduardo Almeida Soares, Sars-CoV-2 CT-scan dataset: A large dataset of real patients CT scans for SARS-CoV-2 identification, MedRxiv (2020).

[5] Jinyu Zhao, Yichen Zhang, Xuehai He, Pengtao Xie, Covid-ct-dataset: a ct scan dataset about covid-19, 2020, arXiv preprint arXiv:2003.13865.

[6] Li Yan, Hai-Tao Zhang, Yang Xiao, Maolin Wang, Yuqi Guo, Chuan Sun, Xiuchuan Tang, et al., Prediction of criticality in patients with severe Covid-19 infection using three clinical features: a machine learning-based prognostic model with clinical data in wuhan, MedRxiv (2020).

[7] Shaoping Hu, Yuan Gao, Zhangming Niu, Yinghui Jiang, Lao Li, Xianglu Xiao, Minhao Wang, et al., Weakly supervised deep learning for covid-19 infection detection and classification from ct images, IEEE Access 8 (2020) 118869-118883.

[8] Jun Chen, Lianlian Wu, Jun Zhang, Liang Zhang, Dexin Gong, Yilin Zhao, Qiuxiang Chen, et al., Deep learning-based model for detecting 2019 novel coronavirus pneumonia on high-resolution computed tomography, Sci. Rep. 10 (1) (2020) 1–11.

[9] Fei Shan, Yaozong Gao, Jun Wang, Weiya Shi, Nannan Shi, Miaofei Han, Zhong Xue, Yuxin Shi, Lung infection quantification of COVID-19 in CT images with deep learning, 2020, arXiv preprint arXiv:2003.04655.

[10] . Yap, Moi Hoon, Gerard Pons, Joan Marti, Sergi Ganau, Melcior Sentis, Reyer Zwiggelaar, Adrian K. Davison, Robert Marti, Automated breast ultrasound lesions detection using convolutional neural networks, IEEE J. Biomed. Health Inf. 22 (4) (2017) 1218–1226.

[11] M.H Hesamian, W Jia, X He, et al., Deep learning techniques for medical image segmentation: achievements and challenges, J. Digit. Imaging 32 (4) (2019) 582–596.

[12] Qing Li, Weidong Cai, Xiaogang Wang, Yun Zhou, David.Dagan Feng, Mei Chen, Medical image classification with convolutional neural network, in: 2014 13th International Conference on Control Automation Robotics & Vision (ICARCV), IEEE, 2014, pp. 844–848.

[13] Marios Anthimopoulos, Stergios Christodoulidis, Lukas Ebner, Thomas Geiser, Andreas Christe, Stavroula Mougiakakou, Semantic segmentation of pathological lung tissue with dilated fully convolutional networks, IEEE J. Biomed. Health Inf. 23 (2) (2018) 714–722.

[14] William S. Noble, What is a support vector machine? Nature Biotechnol. 24 (12) (2006) 1565–1567.

[15] Leo Breiman, Random forests, Mach. Learn. 45 (1) (2001) 5–32.

[16] D.G Kleinbaum, K Dietz, M Gail, et al., Logistic Regression, Springer-Verlag, New York, 2002.

[17] M.H. Hassoun, Fundamentals of Artificial Neural Networks, MIT Press, 1995.

[18] Ruey-Feng Chang, Wen-Jie Wu, Woo.Kyung Moon, Yi-Hong Chou, Dar-Ren Chen, Support vector machines for diagnosis of breast tumors on US images, Acad. Radiol. 10 (2) (2003) 189–197.

[19] Gustavo Carneiro, Jacinto Nascimento, Andrew P. Bradley, Unregistered multiview mammogram analysis with pre-trained deep learning models, in: International Conference on Medical Image Computing and Computer-Assisted Intervention, Springer, Cham, 2015, pp. 652–660.

[20] Nima Tajbakhsh, Kenji Suzuki, Comparing two classes of end-to-end machine-learning models in lung nodule detection and classification: MTANNs vs. CNNs, Pattern Recognit. 63 (2017) 476–486.

[21] . Ayhan, Murat Seckin, Philipp Berens, Test-time data augmentation for estimation of heteroscedastic aleatoric uncertainty in deep neural networks, 2018.

[22] Subhankar Roy, Willi Menapace, Sebastiaan Oei, Ben Luijten, Enrico Fini, Cristiano Saltori, Iris Huijben, et al., Deep learning for classification and localization of COVID-19 markers in point-of-care lung ultrasound, IEEE Trans. Med. Imaging 39 (8) (2020) 2676–2687.

[23] Shome, Debaditya, et al., COVID-Transformer: Interpretable COVID-19 detection using vision transformer for healthcare, Int. J. Environ. Res. Public Health 18 (21) (2021) 11086.

[24] K Shankar, et al., An optimal cascaded recurrent neural network for intelligent COVID-19 detection using chest X-ray images, Appl. Soft Comput. 113 (2021) 107878.
[25] Abbas Mardani, Robert E. Hooker, Seckin Ozkul, Sun Yifan, Mehrbakhsh Nilashi, Hamed Zamani Sabzi, Goh Chin Fei, Application of decision making and fuzzy sets theory to evaluate the healthcare and medical problems: a review of three decades of research with recent developments, Expert Syst. Appl. 137 (2019) 202–231.
[26] Rikalovic Aleksandar, Ilija Cosic, Ruggero.Donida Labati, Vincenzo Piuri, Intelligent decision support system for industrial site classification: A GIS-based hierarchical neuro-fuzzy approach, IEEE Syst. J. 12 (3) (2017) 2970–2981.
[27] Sousa, MC. João, Susana M. Vieira, João P. Carvalho, Sara C. Madeira, Leo Celi, Stan N. Finkelstein, An architecture based on fuzzy systems for personalized medicine in ICUs, in: 2019 IEEE International Conference on Fuzzy Systems (FUZZ-IEEE), IEEE, 2019, pp. 1–6.
[28] Shuofang Liu, Juan Li, Zhe Li, Fuzheng Zhao, Performance evaluation of design courses based on fuzzy decision-making method, in: 2019 International Joint Conference on Information, Media and Engineering (IJCIME), IEEE, 2019, pp. 284–287.
[29] Chenyang Song, Yixin Zhang, Zeshui Xu, Zhinan Hao, Xinxin Wang, Route selection of the arctic northwest passage based on hesitant fuzzy decision field theory, IEEE Access 7 (2019) 19979–19989.
[30] Xiaonan Xiao, Establishment and application of a class of fuzzy decision-making model for optimal diagnosis and determination of diseases, in: 2020 12th International Conference on Measuring Technology and Mechatronics Automation (ICMTMA), IEEE, 2020, pp. 523–525.
[31] Gabriella Casalino, Riccardo Grassi, Marco Iannotta, Vincenzo Pasquadibisceglie, Gianluca Zaza, A hierarchical fuzzy system for risk assessment of cardiovascular disease, in: 2020 IEEE Conference on Evolving and Adaptive Intelligent Systems (EAIS), IEEE, 2020, pp. 1–7.
[32] Khomeiny, Akrom Tegar, Tegar Restu Kusuma, Anik Nur Handayani, Aji Prasetya Wibawa, Agus Hery Supadmi Irianti, Grading system recommendations for students using fuzzy mamdani logic, in: 2020 4th International Conference on Vocational Education and Training (ICOVET), IEEE, 2020, pp. 1–6.
[33] Sadiq H. Abdulhussai, et al., A fast feature extraction algorithm for image and video processing, in: 2019 International Joint Conference on Neural Networks (IJCNN), IEEE, 2019.
[34] Abderrazak Chahid, et al., A position weight matrix feature extraction algorithm improves hand gesture recognition, in: 2020 42nd Annual International Conference of the IEEE Engineering in Medicine & Biology Society (EMBC), IEEE, 2020.
[35] Alessandro S. Martins, et al., Colour feature extraction and polynomial algorithm for classification of lymphoma images, in: Iberoamerican Congress on Pattern Recognition, Springer, Cham, 2019.
[36] Mohamed Bennasar, Yulia Hicks, Rossitza Setchi, Feature selection using joint mutual information maximisation, Expert Syst. Appl. 42 (22) (2015) 8520–8532.
[37] Weihao Zheng, et al., Multi-feature based network revealing the structural abnormalities in autism spectrum disorder, IEEE Trans. Affect. Comput. (2019).
[38] Chuanze Kang, et al., Feature selection and tumor classification for microarray data using relaxed lasso and generalized multi-class support vector machine, J. Theoret. Biol. 463 (2019) 77–91.
[39] S.P Morozov, et al., Mosmeddata: Chest ct scans with covid-19 related findings dataset, 2020, arXiv preprint arXiv:2005.06465.
[40] Yifan Peng, et al., COVID-19-CT-CXR: A freely accessible and weakly labeled chest X-ray and CT image collection on COVID-19 from biomedical literature, 2020, arXiv preprint arXiv:2006.06177.
[41] Tawsifur Rahman, et al., Exploring the effect of image enhancement techniques on COVID-19 detection using chest X-ray images, Comput. Biol. Med. 132 (2021) 104319.
[42] David G. Lowe, Object recognition from local scale-invariant features, in: Proceedings of the Seventh IEEE International Conference on Computer Vision, Vol. 2, Ieee, 1999, pp. 1150–1157.
[43] Navneet Dalal, Bill Triggs, Histograms of oriented gradients for human detection, in: 2005 IEEE Computer Society Conference on Computer Vision and Pattern Recognition (CVPR'05), Vol. 1, Ieee, 2005, pp. 886–893.
[44] Timo Ojala, Matti Pietikainen, Topi Maenpaa, Multiresolution gray-scale and rotation invariant texture classification with local binary patterns, IEEE Trans. Pattern Anal. Mach. Intell. 24 (7) (2002) 971–987.
[45] Yann LeCun, Léon Bottou, Yoshua Bengio, Patrick Haffner, Gradient-based learning applied to document recognition, Proc. IEEE 86 (11) (1998) 2278–2324.
[46] Alex Krizhevsky, Ilya Sutskever, Geoffrey E. Hinton, Imagenet classification with deep convolutional neural networks, Adv. Neural Inf. Process. Syst. 25 (2012) 1097–1105.
[47] P Kalaiarasi, P. Esther Rani, Comparative analysis of AlexNet and GoogLeNet with a simple DCNN for face recognition, in: Advances in Smart System Technologies, Springer, Singapore, 2021, pp. 655–668.
[48] Qinghua Hu, Daren Yu, Jinfu Liu, Congxin Wu, Neighborhood rough set based heterogeneous feature subset selection, Inform. Sci. 178 (18) (2008) 3577–3594.
[49] Zijun Zhang, Improved adam optimizer for deep neural networks, in: 2018 IEEE/ACM 26th International Symposium on Quality of Service (IWQoS), IEEE, 2018.
[50] Karen Simonyan, Andrew Zisserman, Very deep convolutional networks for large-scale image recognition, 2014, arXiv preprint arXiv:1409.1556.
[51] Christian Szegedy, et al., Going deeper with convolutions, in: Proceedings of the IEEE conference on computer vision and pattern recognition. 2015.
[52] Kaiming He, Xiangyu Zhang, Shaoqing Ren, Jian Sun, Deep residual learning for image recognition, in: Proceedings of the IEEE conference on computer vision and pattern recognition, 2016, pp. 770–778.
[53] Mingxing Tan, Quoc Le, Efficientnet: Rethinking model scaling for convolutional neural networks, in: International Conference on Machine Learning, PMLR, 2019, pp. 6105–6114.
[54] Gao Huang, Zhuang Liu, Laurens Van Der Maaten, Kilian Q. Weinberger, Densely connected convolutional networks, in: Proceedings of the IEEE conference on computer vision and pattern recognition, 2017, pp. 4700–4708.
[55] Pan, Sinno Jialin, Qiang Yang, A survey on transfer learning, IEEE Trans. Knowl. Data Eng. 22 (10) (2009) 1345–1359.
[56] Kaiming He, Haoqi Fan, Yuxin Wu, Saining Xie, Ross Girshick, Momentum contrast for unsupervised visual representation learning, in: Proceedings of the IEEE/CVF Conference on Computer Vision and Pattern Recognition, 2020, pp. 9729–9738.
[57] Hasan Polat, et al., Automatic detection and localization of COVID-19 pneumonia using axial computed tomography images and deep convolutional neural networks, Int. J. Imaging Syst. Technol. 31 (2) (2021) 509–524.
[58] Ying Song, et al., Deep learning enables accurate diagnosis of novel coronavirus (COVID-19) with CT images, IEEE/ACM Trans. Comput. Biol. Bioinform. (2021).
[59] Xuehai He, et al., Sample-efficient deep learning for COVID-19 diagnosis based on CT scans, Medrxiv (2020).
[60] Cosimo Ieracitano, et al., A fuzzy-enhanced deep learning approach for early detection of Covid-19 pneumonia from portable chest X-ray images, Neurocomputing (2022).